JOURNAL OF DEGRADED AND MINING LANDS MANAGEMENT
Volume 9, Number 1 (October 2021): 3137-3154, doi:10.15243/jdmlm.2021.091.3137
ISSN: 2339-076X (p); 2502-2458 (e), www.jdmlm.ub.ac.id

Research Article

Spatial distribution of soil morphology and physicochemical properties to assess land degradation under different NDVI and TRI in North Halmahera, Indonesia

Rofita[1], Sri Nuryani Hidayah Utami[2*], Azwar Maas[2], Makruf Nurudin[2]

[1] Doctoral Program in Agricultural Science, Faculty of Agriculture, Universitas Gadjah Mada, Yogyakarta 55281, Indonesia
[2] Department of Soil Science, Faculty of Agriculture, Universitas Gadjah Mada, Yogyakarta 55281, Indonesia

[*]corresponding author: nuryani@ugm.ac.id

Article history:
Received 29 July 2021
Accepted 28 August 2021
Published 1 October 2021

Keywords:
land degradation
NDVI
soil morphology
soil physicochemical
TRI

Abstract

Land degradation is currently a major environmental problem that can lead to decreasing biomass productivity. The causes of land degradation have been widely reported. However, the soil morphological characteristics and its detailed properties related to land degradation need to be investigated further. The research was conducted in North Halmahera Regency in March-April 2020. The study started with an overlay of basic maps such as rainfall, land use, topography, and soil types to map the degraded land units. Several land units classified from slightly damaged to severely damaged will be validated based on field observations and supported by laboratory measurements. Characterization of soil morphology and soil sampling was carried out according to USDA international standards. Sentinel 2A image and SRTM image from March to April 2020 were used to determine NDVI and TRI. The characteristics of the soils that have not been degraded tend to be found in volcanic landscapes, while those of the degraded soils tend to be found in structural and karst hills. The thickness of the degraded soil horizons tends to be shallower with an incomplete horizon arrangement, and many rock fragments are found in the soil surface layer. SOC gradually decreases in degraded soils, while the essential nutrients (N, P, and K) are relatively more varied across soil types. The improper land use without conservation on steep slopes causes the soils to be easily degraded. The soil degradation index has a linear relationship with NDVI and TRI. Thus, the revitalization of degraded lands needs to pay attention to the layout and types of vegetation with different slope levels according to the geomorphological zone.

To cite this article: Rofita, Utami, S.N.H., Maas, A. and Nurudin, M. 2021. Spatial distribution of soil morphology and physicochemical properties to assess land degradation under different NDVI and TRI in North Halmahera, Indonesia. Journal of Degraded and Mining Lands Management 9(1): 3137-3154, doi: 10.15243/jdmlm.2021.091.3137.

Introduction

Soil degradation is often associated with the loss of soil ability to provide services to the surrounding ecosystem. The loss of soil ability is preceded by an imbalance of the soil properties, including physical, chemical, and biological properties (Jie et al., 2002; Kooch et al., 2020). The soil physical properties provide a place to support the plant body and pass water (Koutný et al., 2014). The function of soil chemical properties can be related to the supply of nutrients, especially macro essential for plants (Khaled and Fawy, 2011). Meanwhile, the soil biological properties provide a place for the growth of macro-mesofauna and soil microorganisms that decompose organic matter (Frouz et al., 2008). The balance between the soil physical, chemical, and biological properties indicates that the soil can support the

ecosystem and provide a place for plant biomass to grow (Li et al., 2021). One of the main problems to increase biomass productivity in agriculture is soil degradation (Li et al., 2021). Soil degradation decreases the productivity of plant biomass and plant diversity (Zhumanova et al., 2018). Besides, land degradation also causes some problems in the socio-economic community, including a decrease in the community income.

In tropical areas such as Indonesia, climate plays an important role in accelerating soil degradation in areas with inappropriate soil management. Besides, geological factors also have a strong influence in certain areas, such as in the North Halmahera Regency. The boundaries of geological factors are influenced by the shape and process so that under certain conditions, it accelerates soil development and vice versa, also inhibits soil development. Geological processes affect the formation of different landforms, including volcanic, uplifting, and sedimentation, which cause differences in terms of land topography. Topography determines drainage density, slope gradient, and surface water flow velocity (Sun et al., 2014). Besides, slope length and steepness are associated with water runoff and soil erosion (Chaplot et al., 2005). Climate and topography are the main natural drivers of soil degradation. Another factor that plays a role in soil degradation is anthropogenic factors, one of which is land use conversion (Wessels et al., 2004). The land use conversion changes vegetation density and diversity, exposes surface soils, triggers erosion, and accelerates soil degradation.

Land use planning and management are the key factors for reducing soil degradation. Conservation techniques on steep slopes, improvement of soil with water and nutrient retention, and provision of organic matter and microorganisms are efforts that can be made to reduce soil degradation and improve soil quality (Noviyanto et al., 2017). Many previous researchers in Indonesia have conducted soil degradation assessments (Widiatiningsih et al., 2018; Aji et al., 2020; Mujiyo et al., 2020), but few have combined the linkages between soil degradation and NDVI and TRI. Zhumanova et al. (2018) used NDVI to determine degraded vegetation types, while Noviyanto et al. (2020) used TRI to determine land degradation threats such as erosion and landslides. The method for mapping the soil degradation index based on the detailed distribution of soil morphological and physicochemical characteristics needs to be further developed.

Materials and Methods

Study area and soil sampling

The research was conducted in North Halmahera Regency (area 347,693.37 km^2) from March to April 2020. In general, the rainfall in Halmahera Regency is around 2,500-3,000 mm, where the distribution of rainfall can be seen in Figure 1A. The land use is dominated by forest by 53%, followed by mixed gardens by 20%, shrubs by 12%, moor by 10%, and others by 5%. In more detail, the land use in the North Halmahera Regency is presented in Figure 1B. The topography in the study area is also very varied (Figure 1C), in which the slope from steep to very steep is 46%. Meanwhile, Inceptisols tend to dominate soil types with an area of >50% (Figure 1D).

Base maps of rainfall, land use, slope, and soil type (Figure 1) with the same scale requirements were overlaid to determine the map of potential soil degradation (Figure 2). Sampling was done on soil degradation with the criteria slightly damaged to very damaged, where both have an area requirement of >100 ha. Fifteen soil profiles were obtained, and the data were used to validate the map of potential soil degradation. Detailed information from the 15 profiles is presented in Table 1. Land slope and land use are the determinants of soil degradation. There are 13 soil profiles found on steep to very steep terrain and two soil profiles on gentle slopes but are classified as floodplains (fluvial). Land uses that are still natural (forest and secondary forest) have four soil profiles, while the lands that have been converted (gardens, mixed gardens, and moor) have 11 soil profiles.

Fieldwork and laboratory measurements

The fieldwork was carried out according to the international standard USDA soil description (Schoeneberger et al., 2012) that consisted of landscape and soil profile observations. The variables of landscape observation include coordinates, elevation, slope, position and direction of slopes, land use, vegetation type, and land conservation. Meanwhile, the soil profile observations consisted of qualitative and quantitative observations. Qualitative observations include the determination of soil horizonization, soil depth, soil horizon boundaries based on the level of change and shape, soil colour, soil structure (degree of hardness, size, and shape), soil consistency (wet conditions), and plant roots (number and size). Quantitative observations include the analysis of physicochemical properties of the soil, measured by taking soil samples continuously. The analysis methods related to soil physicochemical parameters adjusted to standard laboratory procedures (van Reeuwijk, 2002) are presented in Table 2.

Data analysis

The parameters for determining the soil degradation index were based on Government Regulation No. 150 of 2000 combined by previous researchers (Aji et al., 2020), including rainfall, slope, land conservation, land use, flooding, pH, electrical conductivity, soil depth, surface rock, and sand fraction. Several other researchers also used the same method (Widiatiningsih et al., 2018; Mujiyo et al., 2020) in determining the potential of soil degradation.

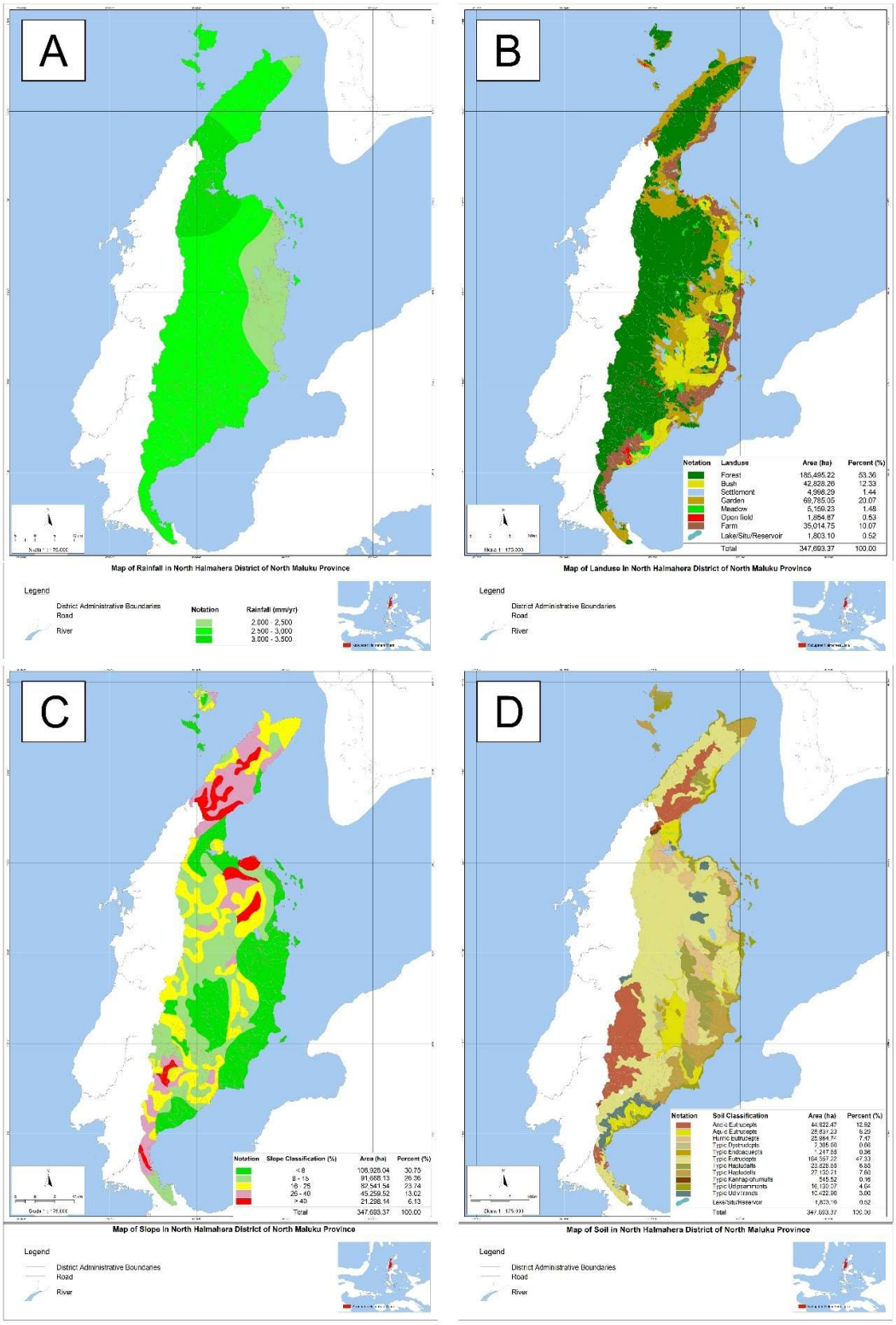

Figure 1. Base map: (A) climate, (B) land use, (C) topography, (D) soil type.

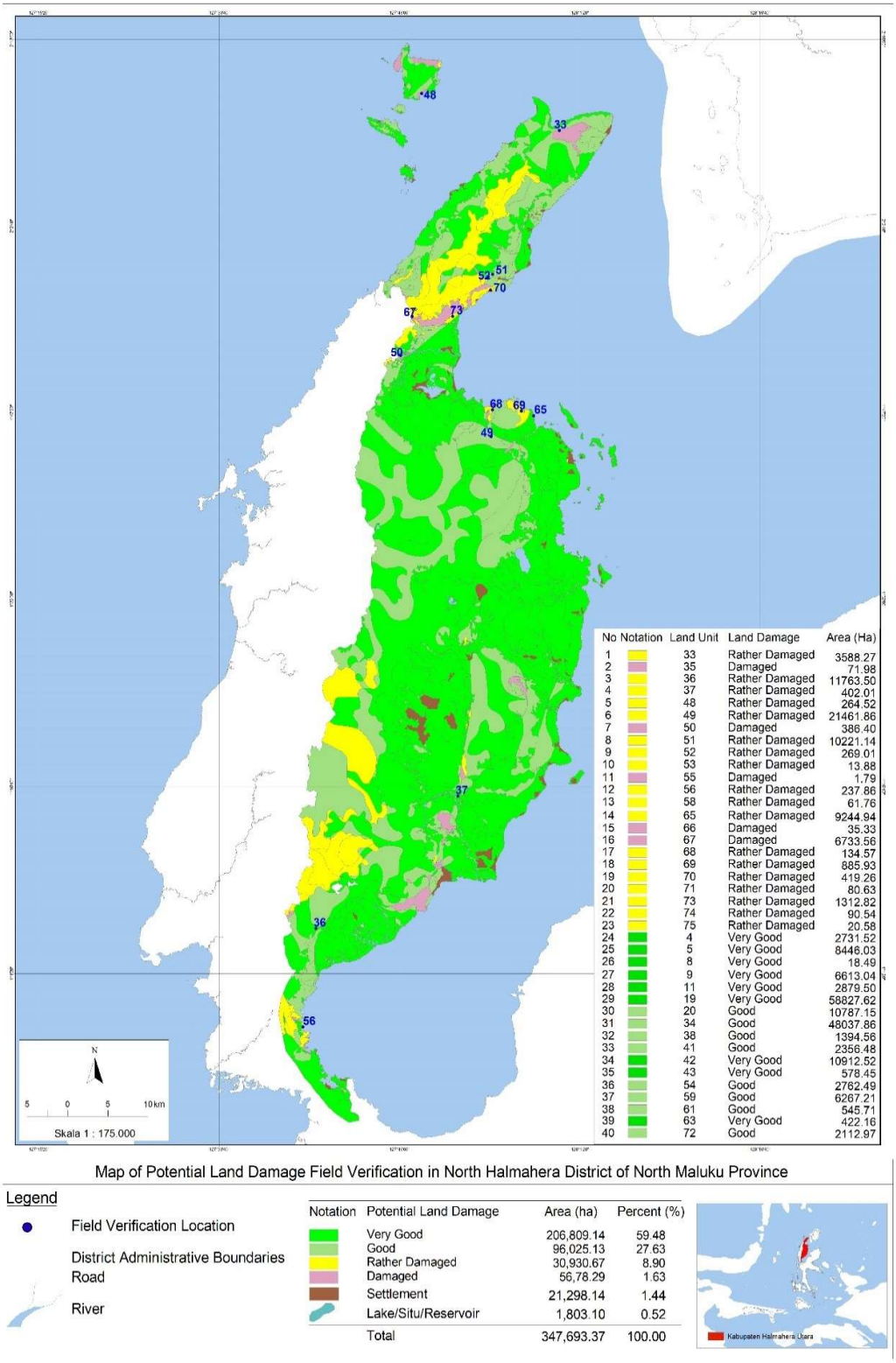

Figure 2. Potential of soil degradation.

Table 1. Characteristics of the area studied.

Soil profile	Coordinates		Location	Elevation (m asl)	LF	GF	PM	GU	Slope (%)	LU	Vegetation
	Latitude	Longitude									
P65	120º57′24.5″	01º43′05.4″	Gosoma, Tobelo	272	M	Qhva	VA	C	47	F	Bamboo, Nutmeg
P69	120º56′21.1″	01º47′29.5″	Ruko, Tobelo	35	H	Qhva	AB	LS	55	DL	Coconut, Banana, Fits, Groundnut
P68	127º53′53.6″	01º47′34.4″	Mamuya, Tobelo	15	P	Qa	MB	F	0	G	Coconut
P49	120º53′46.7″	01º45′23.7″	Mamuya, Tobelo	166	M	Qpt	VA	US	40	MC	Coconut, Nutmeg
P50	127º46′05.5″	01º52′03.3″	Roko, West Galela	30	P	Tomb	B	LS	30	MC	Coconut, Nutmeg, Langsat
P33	127º59′34.6″	02º10′30.4″	Supu, North Loloda	12	H	Ql	M	LS	70	MC	Coconut, Nutmeg, Banana, Langsat
P70	127º53′43.8″	01º57′24.2″	Bobisiongo, North Galela	22	H	Tomb	A	LS	69	MC	Coconut, Nutmeg, Banana
P51	127º53′54.6″	01º58′41.6″	Bobisiongo, North Galela	35	H	Tomb	BA	MS	79	MC	Coconut, Nutmeg, Banana
P52	127º53′31.6″	01º58′29.8″	Bobisiongo, North Galela	38	H	Tomb	BA	F	0	MC	Coconut, Bamboo, Mango
P73	127º50′30.6″	01º55′15.1″	Limau, North Galela	18	H	Tomb	BA	LS	79	DL	Palm, Banana, Bamboo
P48	127º47′53.2″	02º13′32.6″	Dama, Loloda Islands	21	H	Tmpw	L	MS	60	MC	Coconut, Nutmeg, Banana, Mango
P67	127º47′04.5″	01º55′13.7″	Makaeling, Kao Teluk	90	H	Tomb	BA	MS	90	SF	Enau, Palm, Banana
P37	127º50′56.9″	01º15′53.4″	Popon, Kao	80	H	Qpk	BA	MS	55	F	Nutmeg, Bamboo, Banana, Enau
P56	127º37′47.0″	00º56′56.9″	Bobisiongo, North Galela	25	H	Qpk	BA	MS	30	MC	Teak, Nutmeg, Banana
P36	127º38′54.2″	01º41′41.8″	Makaeling, Kao Teluk	74	M	Qpk	VA	US	50	SF	Nutmeg, Bamboo

Key :

- Landform (LF) = Mountain (M), Hills (H), Plains (P)
- Geological formation (GF) = Holocene volcanic rocks (Qhva), Alluvium (Qa), Togawa formation (Qpt), Bacan formation (Tomb), Reef limestone (Ql), Weda formation (Tmpw)
- Parent material (PM) = Volcanic ash (VA), Andesitic breccia (AB), Mud and boulders (MB), Breccia (B), Marl (M), Andesitic (A), Breccia andesitic (BA), Limestone (L)
- Geomorphologic unit (GU) = Cone (C), Upper slope (US), Middle slope (MS), Lower slope (LS), Fluvial (F)
- Landuse (LU) = Forest (F), Multiple cropping (MC), Secondary forest (SF), Dry land (DL), Garden (G)

Table 2. Standard procedure for analyzing physicochemical properties of the soil.

Parameters	Sample types	Analytical methods
Bulk density (BD)	Undisturbed	Ring
Particle density (PD)	Disturbed	Pycnometer
Porosity (POR)	Disturbed	Determined from BD with PD
Hydraulic conductivity (HC)	Undisturbed	De Boodt
Particle distribution	Disturbed	Hydrometer
pH	Disturbed	Soil: water suspension (1:5; w/v)
Electrical conductivity (EC)	Disturbed	Soil: water suspension (1:5; w/v)
Soil organic carbon (SOC)	Disturbed	Walkley and Black
Total N (Tot-N)	Disturbed	Spectrophotometry
Potential P_2O_5 (Pot-P)	Disturbed	HCl 25%
Potential K_2O (Pot-K)	Disturbed	HCl 25%
Cation Exchange Capacity (CEC)	Disturbed	Distillation
Exchangeable Aluminum (Ex-Al)	Disturbed	Titration
Exchangeable Hydrogen (Ex-H)	Disturbed	Titration

The ten parameters of the soil degradation index were then scored according to previous researchers (Aji et al., 2020), where the scoring results would be classified as very good (≥46%), good (36-45%), moderate (28-35%), damaged (17-27%), and heavily damaged (<16%). The formula for determining the soil degradation index is presented in equation 1.

$$\text{Soil Degradation Index (SDI)} = \left(\frac{\text{Score 1}}{100} \times \frac{\text{Score 2}}{100} \times \ldots \times \text{i}\right) \times 100\% \quad (1)$$

Note= i is the number of variables

Each land degradation index generated from the 15 soil profiles would be associated with the vegetation index and the land surface roughness index. Radiometric corrected 2A Sentinel satellite images were used to determine the vegetation index through normalized difference vegetation index (NDVI) analysis. Meanwhile, Shuttle Radar Topography Mission (SRTM) satellite images were used to determine the land surface roughness index through the terrain ruggedness index (TRI). The value results for each pixel of the NDVI and TRI images were associated with the soil degradation index to determine the relationship between these three variables. The accuracy in the 2A sentinel pixel was 10 m x 10 m, while that of the SRTM was 30 m x 30 m. NDVI and TRI are commonly used for controlling the land degradation rate because of their relation to land use and topography (Higginbottom and Symeonakis, 2014; Yengoh et al., 2015).

Results

Soil morphological properties

The fifteen soil profiles observed have different morphological properties. In general, the soil profile with a thickness of >100 cm is composed of volcanic parent material that has not weathered or has weathered at a light to advanced intensity. Soil profiles with a thickness of <100 cm firmly adjacent to the C and R horizons indicate a lithological discontinuity. Soil profile P49 (Figure 3) indicates the presence of polypedon, characterized by new volcanic material that hitched a ride on volcanic material that was relatively longer. Differences in soil structure and texture indicate the presence of periodic overlapping material. The soil profile P65 (Figure 3) also indicates that it originates from volcanic material that has not weathered on the surface horizon and gradually weathers on the subsurface horizon.

The difference shown in the material that has not weathered is that it has a loose soil structure, in which there is still fresh volcanic ash, while the colour that gradually turns brown indicates that the volcanic ash has started to rot. Besides, the P65 soil profile (Figure 3) with a Bw2v horizon shows the presence of plintite (Table 3), which is also formed due to the differences in the time of deposition of volcanic material in the past. Soil profile P69 (Figure 3) shows a complete horizonization, starting from A-Bw-Bw/C (Table 3). The presence of a Bw horizon indicates that there is a shift in the horizon that is still weak, or it can be interpreted that land development is still early. The position of the P69 soil profile, which is close to active volcanoes and volcanic breccia bedrock, indicates that the surface layer comes from volcanic ash with the SBK structure shape (Table 3) accompanied by a weak degree of hardness and small size, while the Bw horizon has a better degree of hardness and larger sizes (Table 3). Some soil profiles are in the material deposition zone, as shown in Figure 3, which are soil profiles P68, P50, and P52. Soil profile P68 (Figure 3) indicates a more dominant accumulation of sand, and the relatively dark soil colour indicates that there is a mixture of organic matter with relatively wet soil conditions.

Table 3. Morphological properties of the soil.

Sample code	Soil horizon	Depth (cm)	Horizon boundary	Soil color (moist)		Texture	Structure	Consistence (wet)	Roots
P65	A	0-30	C, S	10YR 2/1	Black	Sandy loam	1, F, GR	Non sticky	1, C
	Bw1	30-70	G, W	10YR 3/2	Very dark greyish brown	Silty loam	1, F, SBK	Non sticky	2, M
	Bw2v	70-110	D, S	10YR 3/3	Dark brown	Sandy loam	1, M, SBK	Slightly sticky	1, F
P69	A	0-43	D, W	10YR 3/1	Very dark grey	Sandy loam	1, F, SBK	Slightly sticky	1, M
	Bw	43-69	D, S	10YR 3/3	Dark brown	Loam	2, M, SBK	Slightly sticky	3, C
	Bw/C	69-110	G, S	10YR 4/3	Brown	Loam	1, F, SBK	Non sticky	1, C
P68	A	0-40	D, S	10YR 2/1	Black	Silty loam	1, F, GR	Non sticky	1, M
P49	1A	0-25	C, S	10YR 2/1	Black	Sandy loam	1, F, SBK	Non sticky	3, C
	1Bw1	25-70	D, S	10YR 3/1	Very dark grey	Silty loam	2, F, SBK	Non sticky	2, C
	1Bw2	70-104	C, W	10YR 3/1	Very dark grey	Loam	2, M, SBK	Slightly sticky	2, M
	2Ab	104-135	C, W	10YR 3/2	Very dark greyish brown	Sandy loam	3, M, PL	Non sticky	1, C
	2Bb	135-150	G, S	10YR 3/2	Very dark greyish brown	Loam	2, M, SBK	Slightly sticky	1, M
P50	1A1	0-10	C, W	10YR 3/1	Very dark grey	Loam	1, M, SBK	Non sticky	3, M
	1A2	10-35	G, W	10YR 6/4	Light yellowish brown	Sandy loam	1, F, SBK	Slightly sticky	3, M
	1A/C	35-60	C, W	10YR 7/4	Very pale brown	Sandy loam	3, CO, PL	Non sticky	3, C
	2A	60-120	G, S	2.5Y 5/1	Grey	Loamy sand	1, F, GR	Non sticky	3, C
P33	A	0-23	C, W	2.5 Y 3/2	Very dark greyish brown	Silty clay loam	2, M, SBK	Slightly sticky	3, C
	A/C	23-120	G, S	2.5 Y 7/3	Pale brown	Silty clay	1, F, SBK	Slightly sticky	1, C
P70	A	0-50	D, W	10YR 2/2	Very dark brown	Clay loam	3, M, SBK	Slightly sticky	3, C
	Bw	50-100	G, S	10YR 3/1	Very dark grey	Clay	3, CO, SBK	Non sticky	2, C
P51	A/C	0-50	D, W	7.5YR 2.5/2	Very dark brown	Loam	2, M, SBK	Slightly sticky	3, C
	Bw/C	50-115	D, W	5YR 2.5/2	Dark reddish brown	Loam	3, M, SBK	Slightly sticky	3, C
P52	1A	0-50	D, W	10YR 5/4	Yellowish brown	Silty loam	1, F, SBK	Non sticky	3, M
	2Ab	50-90	D, S	10YR 5/4	Yellowish brown	Loam	1, M, SBK	Slightly sticky	1, F
	2Bwb	90-120	D, S	10YR 3/4	Dark yellowish brown	Loam	2, M, SBK	Moderately sticky	-
P73	A	0-26	D, W	10YR 2/2	Very dark brown	Loam	2, M, SBK	Moderately sticky	2, M
	Bw/C	26-65	G, W	10YR 3/1	Very dark grey	Clay loam	2, M, SBK	Moderately sticky	1, M
	C	65-200	D, S	10YR 3/1	Very dark grey	Sandy clay loam	1, M, SBK	Slightly sticky	-
P48	A	0-30	C, W	10YR 2/2	Very dark brown	Clay loam	3, M, SBK	Moderately sticky	3, C
	A/C	30-80	C, W	10YR 3/6	Dark yellowish brown	Clay	2, F, SBK	Moderately sticky	2, M
P67	A/C	0-120	D, S	7.5YR 3/4	Dark brown	Loam	2, M, SBK	Slightly sticky	1, C
P37	A	0-50	C, W	7.5YR 3/3	Dark brown	Clay loam	1, M, SBK	Moderately sticky	2, C
	Bt	50-120	D, S	2.5YR 4/6	Red	Clay	2, M, SBK	Very sticky	1, F

Sample code	Soil horizon	Depth (cm)	Horizon boundary	Soil color (moist)		Texture	Structure	Consistence (wet)	Roots
P56	A/C	0-70	C, W	10YR 3/1	Very dark grey	Loam	1, F, SBK	Slightly sticky	3, M
P36	A	0-44	G, W	10YR 3/2	Very dark greyish brown	Clay	1, F, SBK	Slightly sticky	2, M
	Bw1	44-100	D, S	10YR 4/6	Brown	Clay loam	1, F, SBK	Slightly sticky	2, F
	Bw2	100-120	D, S	10YR 4/2	Dark greyish brown	Clay	2, M, SBK	Moderately sticky	1, F

Key:

- Horizon distinctness and topography = Clear (C), Gradual (G), Diffuse (D), Smooth (S); Wavy (W)
- Structure grade, size, and type = Weak (1), Moderate (2), Strong (3), Fine (F), Medium (M), Coarse (CO), Subangular blocky (SBK), Platy (PL), Granular (GR)
- Root quantity and size = Few (1), Common (2), Many (3), Fine (F), Medium (M), Coarse (C)

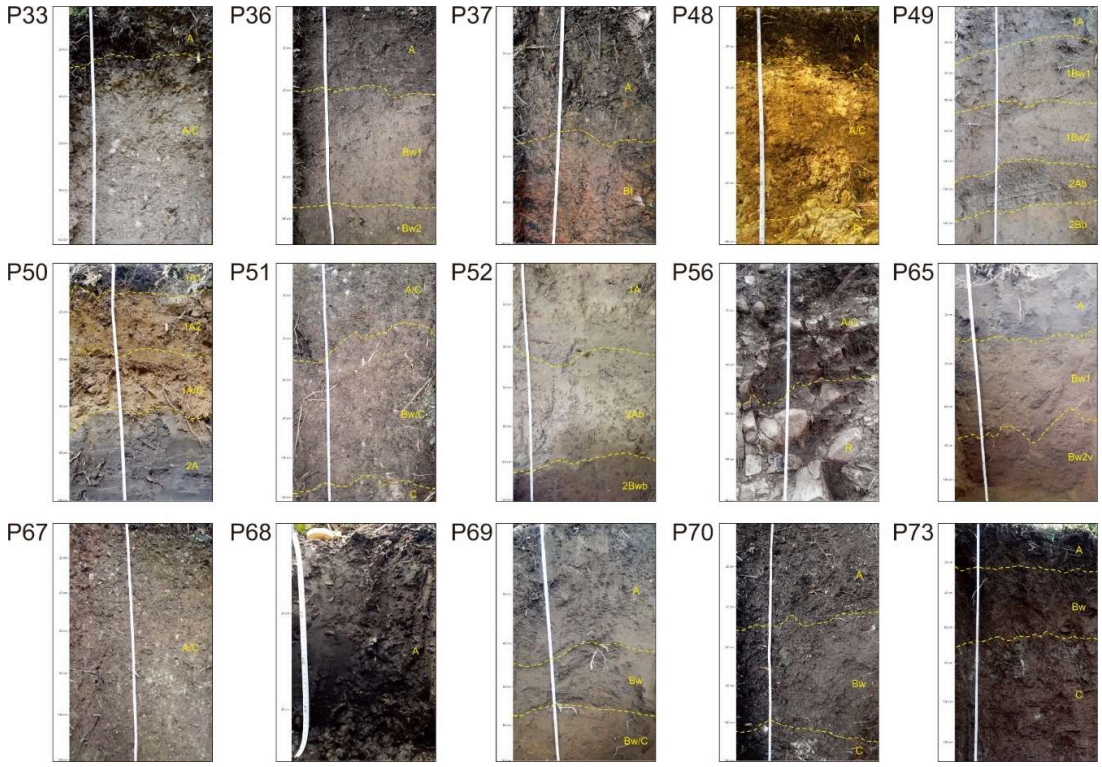

Figure 3. Soil profiles.

Soil profile P50 (Figure 3) illustrates a very clear difference in material, in which the 1A1, 1A2, and 1A/C horizons (Table 3) originate from soil erosion deposits on its upper slopes, and the 2A horizon (Table 3) originates from the river sediments. The topsoil layer tends to be brown in colour with the SBK and PL structures (Table 3), while the subsoil layer tends to be grey in colour with a loose structure and sandy texture (Table 3). Soil profile P52 in Figure 3 also depicts the presence of different sediments resulted from sedimentation. Soil profiles in the material deposition zone generally have SBK soil structures with small sizes so that the soil structure is loose and easily destroyed (Table 3).

Soil profiles on the lower slopes with different parents are shown in soil profiles P33, P70, P51, P73, P48, and P56 (Figure 3). The bedrock in the form of limestone located in karst hills is shown in the soil profiles P33 and P48. Both have distinctively developed soil characteristics, which are dark in colour and relatively soft. Soft soil characteristics lead to the molecular properties of the soil classification system. The dark colour on the surface horizon indicates the presence of relatively high organic matter. The P70 soil profile illustrates further soil development but not further than that of the P73 soil profile. Both have the same soil structure, namely SBK, but the consistency is more sticky, as shown in the soil profile P73 compared to P70. The different soil colour between the P70 and P73 soil profiles is due to the different origin of the parent material, where the P70 soil profile comes from andesite parent material, and the P73 soil profile comes from the andesite breccia parent material. The soil profile P51 illustrates the presence of a mixture of parent material in the form of gravel and scale grains in each A/C-Bw/C-C horizon (Figure 3). The presence of gravels either on the soil surface or in the soil profile can inhibit plant root growth because it is often used as a characteristic of soil degradation. Soil profile P56 in Figure 3 illustrates that large rocks dominate the A/C horizon and R horizon. The relatively small number and size of plant roots indicate that plant roots cannot penetrate rocks, and only certain plants can grow adaptively.

The soil profile found on the middle slope has a relatively thick A horizon of 30-50 cm (Table 3), as shown in soil profiles P67, P37, and P36 (Figure 3). Soil profile P36 is located in the mountains close to volcanic areas so that there is still an enrichment of volcanic material that has weathered to form the SBK structure (Table 3). The gradation of gradual change in colour from dark brown to brown indicates control of organic matter on the surface horizon and clay illuviation on the subsurface horizon. Soil profile P37 illustrates the presence of the Bt horizon, which belongs to the argillic horizon (Table 3). The argillic horizon indicates enrichment in the percentage of clay in the subsurface layer. Soil profile P67 only has one horizon in the form of A/C, which is thick enough to 60 cm (Table 3).

Soil physicochemical properties

Soil profiles originating from weathered volcanic ash are P65, P69, P49, and P36. The four profiles have different levels of soil development, where the soil profiles of P65, P69, and P49 tend not to weather because the percentage of clay content is relatively lower (<10%) compared to the P36 soil profile, which contains a percentage of clay >30% (Table 4).

The distribution of soil particle size can affect the speed of soil in passing water. The permeability in the soil profiles P65, P69, and P49 tend to be rather fast (HC > cm/h) compared to that in P36 soil profiles, which is very slow (HC <0.1 cm/h) (Table 4). There are no significant differences in the bulk density and porosity of the soil profiles P65, P69, P49, and P36 (Table 4). The pH (H_2O) in the soil profiles P65 and P69 tends to be neutral with a pH value >6.5, while in the soil profile P49, it tends to be slightly acidic with a pH value <6.5 (Table 4). In contrast to the three profiles, the soil profile P36 has a varying pH in each horizon, which tends to get more acidic as the depth of the soil horizon increases (Horizon A-Bw1-Bw2/pH 6.37, 5.66, 4.97).

Organic C in the soil profiles P65, P69, P49, and P36 is low (<2%), which causes the soil to be prone to degradation. The essential nutrients (N, P, and K) in the soil have an important role in providing nutrients for plants. The total N content in the soil profiles P65, P69, P49, and P36 tends to be low (<2%), while the P-potential and K-potential tend to vary (Table 4). Soil profiles P65, P69, and P49 tend to contain low CEC values (<17 cmol(+)/kg), whereas the soil profile P36 tends to contain varied CEC values in each soil horizon (horizon A-Bw1-Bw2 / CEC 8.61 cmol(+)/kg, 28.99 cmol (+)/kg, 18.51 cmol(+)/kg).

Soil profiles that are affected by the sedimentation process of other materials are shown in the soil profiles P68, P50, and P52. The three profiles have different characteristics, according to the material transfer process and material origin. In the soil profile P68, there is only horizon A, composed of silt mixed with sand sediment (Table 4). The percentage of sand and dust particles is more dominant, with the amount of 39% and 54%, respectively. Whereas in the soil profile P50, the percentage of sand is more dominant than dust and clay, with an average of> 50% (Table 4). The soil profile P52 shows that the size distribution of soil particles tends to vary in each horizon. Soil permeability in soil profile P68 tends to be rather slow (<2 cm/h), in contrast to that in the soil profiles P50 and P52, which tend to be rather fast (>6 cm/h) (Table 4). Bulk density in the soil profile P68 tends to be higher than that in the soil profiles P50 and P52 soil profiles, illustrating that the soil profile P68 is denser (Table 4).

Soil chemical properties that are significant to distinguish soil profiles P68, P50, and P52 are soil pH and CEC, in which these two parameters are correlated. The pH (H_2O) in the soil profile P68 is classified as very acidic because the pH value is <4, while the soil profile P50 is classified as neutral with an average pH value of 6.5, and the soil profile P52 is classified as slightly alkaline because the pH value is >7.6 (Table 4). CEC values in the the soil profiles P68, P50, and P52 also differ, classified as very low (<5 cmol(+)/kg), low (<16 cmol(+)/kg), and high (>35 cmol (+)/kg), consecutively. The difference in pH and CEC indicates the origin of different sedimentation materials. Other soil chemical properties do not have a significant difference. The soil degradation indicator, which is soil organic c, also shows a low average value for the three soil profiles, except for the P50 surface horizon, which tends to be high (Table 4).

Soil profiles P33 and P48 have similarities derived from weathered marl and limestone rocks with almost similar rock properties. Both profiles have high soil particle sizes (>30%), thus giving relatively soft soil morphological properties. The soil permeability in the soil profiles P33 and P48 is moderate to quite fast, both of which are due to the high percentage of dust (>30%) in the soil profile P33 and the high percentage of sand (> 30%) in the soil profile P48 (Table 4). Meanwhile, the chemical properties of the two profiles have a pH that tends to be neutral. However, the CEC tends to be higher in the soil profile P33 than in P48. Soil organic C and total N content are higher in the soil profile P48 compared to in the soil profile P33. Conversely, the content of potential P and K is higher in the soil profile P33 compared to P48 (Table 4).

Soil profiles located in the Bacan geological formation (Tomb) with rock characteristics in the form of breccias and lava composed of andesite and basalt are P70, P51, P73, and P67. The four profiles have different soil physicochemical properties, possibly due to the influence of the hilly topography. The four profiles have almost the same texture in the loam class, and some in combination with sandy clay loam and clay loam (Table 4). The balanced distribution of particles between sand, dust, and clay resulted in the loam soil texture class. The permeability in the soil profiles P51, P73, and P70 is relatively slower than that in the soil profile P70, in which the soil profile still contains rock fragments combined with a high percentage of sand, thereby increasing the soil's ability to pass water.

The soil pH in the four profiles is classified as neutral (6.5<pH<7.5). However, the CEC in each profile varies greatly (Table 4). The soil profiles P70 and P51 have higher CEC compared to P73 and P67. The four profiles have a higher potential K compared to the potential P. Meanwhile, there was no significant difference in the soil organic C and total N content (Table 4). Soil profile P37 has a level of soil development that is more intense compared to other soil profiles, seen from the formation of an argillic horizon characterized by the presence of cutaneous crystals and a percentage of clay particles of 71% (Table 4).

Table 4. Soil physicochemical properties.

Soil Profile	Soil horizon	Particle distribution (%)			HC (cm/h)	BD (g/cc)	PD (g/cc)	POR (%)	pH	EC (µs/cm)	SOC (%)	N-tot (%)	P-pot (mg/100g)	K-pot (mg/100g)	CEC (cmol(+)/kg)	Ex-Al (me/100g)	Ex-H (me/100g)
		Sand	Silt	Clay													
P65	A	53	40	7	7.78	1.30	2.71	52.07	6.98	32	0.95	0.18	83	7	2.01	0.00	0.04
	Bw1	43	52	5	8.43	1.05	2.48	57.77	6.91	33	1.47	0.22	44	22	8.49	0.00	0.27
	Bw2v	50	43	7	-	0.90	2.35	61.49	6.65	41	1.13	0.10	16	58	17.65	0.00	0.07
P69	A	51	42	7	6.33	1.05	2.38	55.93	7.67	34	1.76	0.26	112	234	12.50	0.00	0.02
	Bw	53	38	9	10.45	0.94	2.30	59.08	7.09	34	0.96	0.13	57	106	14.38	0.00	0.26
	Bw/C	46	44	9	-	1.05	2.55	58.72	6.97	90	0.89	0.16	52	123	17.39	0.00	0.41
P68	A	39	54	7	1.20	1.21	2.51	51.80	3.99	25	1.11	0.08	80	12	4.74	0.00	0.83
P49	1A	55	38	7	12.13	1.23	2.68	54.09	6.09	51	1.27	0.17	84	7	2.61	0.00	0.38
	1Bw1	38	55	7	8.16	1.13	2.58	56.08	6.23	43	1.42	0.34	38	11	8.81	0.00	0.53
	1Bw2	46	45	9	-	1.12	2.60	57.12	6.59	38	1.00	0.16	25	13	7.73	0.00	0.31
	2Ab	59	36	5	-	0.84	2.16	60.92	6.48	47	0.62	0.03	23	23	5.86	0.00	0.14
	2Bb	52	39	9	-	0.94	2.63	64.15	6.45	93	0.92	0.16	39	27	9.79	0.00	0.35
P50	1A1	51	39	10	17.10	0.86	2.17	60.49	6.63	31	3.40	0.97	14	91	15.52	0.00	0.41
	1A2	47	46	7	7.13	0.97	2.50	61.45	6.43	31	1.37	0.35	38	34	11.95	0.00	0.73
	1A/C	64	29	7	-	0.90	2.52	64.24	6.45	14	0.84	0.11	45	32	8.56	0.00	1.10
	2A	78	17	5	-	1.34	2.77	51.58	6.60	13	0.62	0.02	39	8	0.80	0.00	0.04
P33	A	17	44	39	10.88	0.87	2.09	58.45	7.32	240	2.64	0.61	105	95	43.01	0.00	0.09
	A/C	10	45	45	2.91	0.81	2.44	66.91	7.61	123	1.08	0.18	63	34	27.33	0.00	0.54
P70	A	21	39	39	3.49	1.06	2.00	46.92	7.20	46	1.90	0.32	11	56	28.38	0.00	0.07
	Bw	21	33	46	3.63	1.06	2.62	59.76	7.00	48	1.49	0.22	14	47	40.04	0.00	0.09
P51	A/C	43	36	21	0.75	1.11	2.63	57.64	6.80	36	1.43	0.39	25	83	55.15	0.00	0.09
	Bw/C	41	36	23	0.25	1.09	2.75	60.51	6.85	39	1.42	0.49	38	76	37.39	0.00	0.15
P52	1A	36	51	14	14.47	1.05	2.64	60.05	7.81	23	0.77	0.10	94	31	38.33	0.00	0.06
	2Ab	49	35	16	2.06	1.17	2.63	55.55	7.76	56	0.89	0.29	75	27	37.50	0.00	0.49
	2Bwb	35	42	22	-	1.11	2.27	55.15	7.73	33	0.94	0.33	54	22	17.20	0.00	0.24
P73	A	44	32	23	0.02	1.08	2.47	56.44	6.91	60	2.11	0.39	18	65	17.80	0.00	0.00
	Bw/C	29	32	39	0.13	1.12	2.60	56.44	7.19	24	1.12	0.21	6	38	34.14	0.00	0.57
	C	48	25	27	-	1.24	2.59	52.12	7.07	23	0.59	0.10	19	58	27.52	0.00	0.22
P48	A	41	27	32	3.45	1.01	2.36	57.36	7.07	25	3.97	0.75	28	46	16.44	0.00	0.30
	A/C	42	5	53	4.92	0.98	2.49	60.52	6.35	31	1.33	0.25	18	9	28.60	0.00	0.30
P67	A/C	51	33	16	9.41	1.10	2.42	54.56	6.95	6	1.28	0.28	59	66	14.60	0.00	0.00
P37	A	21	44	35	0.34	1.02	2.48	58.75	5.44	49	2.58	0.57	20	14	12.06	0.00	0.11
	Bt	4	25	71	0.41	0.99	2.35	57.88	5.12	133	1.47	0.19	11	12	11.01	0.00	0.31
P56	A/C	45	35	21	0.36	1.02	2.27	55.15	7.67	20	3.27	0.84	21	22	19.70	0.00	0.26

Soil Profile	Soil horizon	Particle distribution (%)			HC (cm/h)	BD (g/cc)	PD (g/cc)	POR (%)	pH	EC (μs/cm)	SOC (%)	N-tot (%)	P-pot (mg/100g)	K-pot (mg/100g)	CEC (cmol(+)/kg)	Ex-Al (me/100g)	Ex-H (me/100g)
		Sand	Silt	Clay													
P36	A	23	33	44	0.78	1.03	2.35	56.37	6.37	25	1.98	0.47	26	15	8.61	0.00	0.17
	Bw1	24	37	39	0.49	1.10	2.14	48.49	5.66	24	1.16	0.20	17	15	28.99	0.00	0.17
	Bw2	14	38	48	-	1.08	2.60	58.61	4.97	66	1.14	0.15	8	17	18.51	0.00	0.06

The percentage of clay, which tends to be high in the soil profile P37, results in the slow soil permeability to <0.5 cm/h (Table 4). One of the soil chemical properties in the soil profile P37 is soil pH, which tends to be acidic with low CEC. Meanwhile, the organic C, total N, potential P, and potential K in the surface horizon are relatively higher than in the subsurface horizon (argillic horizon).

Soil profile P55 has a relatively thin horizon accompanied by a well-defined lithological discontinuity with an R horizon below it. The relatively slow rate of soil development is indicated by a larger percentage of sand compared to dust and clay (Table 4). The characteristic of slow soil permeability is also related to the number of gravel fragments in the soil. However, the chemical properties of the soil provide good potential for plants. Soil pH shows a value of 7.67, classified as slightly alkaline. The soil organic C is high, namely 3.27%, and the total N-soil is also high, with a value of 0.84 (Table 4). However, soil chemical properties such as potential P, potential K, and CEC are in moderate criteria, with values of 21 mg/100g, 22 mg/100g, 19.70 5 cmol(+)/kg, respectively.

Discussion

Each soil type has the potential to experience soil degradation. The rate of soil degradation is controlled by several factors, such as rainfall, topography, land use, and anthropogenic activities with different levels of agitation (Wessels et al., 2004; Núñez-Delgado et al., 2020). Soils originating from volcanic ash will tend to have thick solum with good physicochemical characteristics. The presence of volcanic ash in the soil is able to function in terms of rejuvenating the soil so that it can improve the physicochemical characteristics that have decreased (Aini et al., 2018). Degraded soil is indicated by shallow solum, a high percentage of sand particles, a large presence of surface rock, and poor chemical properties such as soil pH and electrical conductivity for plants. The soil degradation index in the study area is shown in Table 5. The soil degradation index measured in very good class (VF) is shown in the soil profiles P65 and P49, both of which are included in the soil dominated by weathered volcanic ash. Volcanic ash material that has not undergone weathering is present in the surface horizons of both soil profiles. Volcanic ash can significantly repair soils that have started to experience damage (Aini et al., 2019). Meanwhile, the soil degradation index classified as good is shown in the soil profiles P70 and P52. The differences in the characteristics of the degraded soil between P70 and P52 are in the slope and the presence of surface rock. However, the soil profile P70 is caused by a relatively steep slope with a slight inclination of surface rock. On the other hand, the P52 soil profile is caused by a lot of surface rock on a gentle slope. The texture and structure of the soil profile P70 is clay loam and rounded lumps with a high degree of hardness to reduce the impact of erosion on steep slopes (69%).

Table 5. Soil degradation index.

Soil Profile	Rainfall	Slope	Conser-vation	Land use	Flooding	Soil Depth	Sand	Rock	pH	EC	SDI	Class
65	1	0.5	0.01	1	1	1	1	1	1	1	0.500	VF
69	0.8	0.5	0.01	0.8	1	1	1	1	1	1	0.320	M
68	0.8	1	0.01	0.9	0.7	0.8	1	1	0.8	1	0.323	M
49	1	0.6	0.01	0.9	1	1	1	1	1	1	0.540	VF
50	0.8	0.6	0.01	0.9	1	1	1	0.8	1	1	0.346	M
33	0.8	0.5	0.01	0.9	1	0.7	1	0.8	1	1	0.202	D
70	0.8	0.5	0.01	0.9	1	1	1	1	1	1	0.360	F
51	0.8	0.5	0.01	0.9	1	1	1	0.8	1	1	0.288	M
52	0.8	1	0.01	0.9	0.7	1	1	0.8	1	1	0.403	F
73	0.8	0.5	0.01	0.8	1	1	1	0.8	1	1	0.256	D
48	0.8	0.5	0.01	0.9	1	1	1	0.8	1	1	0.288	M
67	0.8	0.5	0.01	1	1	1	1	0.8	1	1	0.320	M
37	0.8	0.5	0.01	1	1	1	1	0.8	1	1	0.320	M
56	0.8	0.6	0.01	0.9	1	1	1	0.8	1	1	0.346	M
36	0.8	0.5	0.01	1	1	1	1	0.8	1	1	0.320	M

Soil profiles P69, P68, P50, P51, P48, P67, P37, P56, and P36 are categorized as slightly damaged (M). Some of the causes of soil degradation in the nine soil profiles include land use, slope, and land conservation. Land on steep slopes accompanied by inappropriate land use and no land conservation measures can increase erosion (Sun et al., 2014). The incidence of soil erosion depends on the geomorphological unit of the land with various slope levels. Splash erosion generally occurs at the top, small grooves erosion on the middle slope to create valley erosion (gully erosion), and sheet and grooves erosion on the lower

slope (Sartohadi et al., 2018). The high intensity of rain transports not only soil material but also rocks with different sizes and weights, depending on the volume and rate of water runoff on the slopes. Degraded soil classified in damaged criteria (D) is shown by the soil profiles P73 and P33, in which the lowest soil degradation index value is shown by the soil profile P33.

In the soil profile P73, there is a land use in the form of moor, which is not proper, on a steep slope (79%), while the soil profile P33 has shallow soil solum. The absence of ground cover on steep slopes in the soil profile P73 allows the intensity of soil erosion to continue. Uncontrolled soil erosion on steep slopes can result in landslides on a small to large scale (Noviyanto et al., 2020). The shallow soil solum in the soil profile P73 causes the plant roots to be limited in obtaining nutrients and extending the roots so that plants collapse easily (Zhumanova et al., 2018).

The result of the soil degradation index calculation was used to validate the map of potential soil degradation. Validation is necessary because it is possible to correct errors and increase the accuracy of the map. Changes in the soil degradation index were found in the slightly damaged criteria, namely the soil profiles P65 and P49, classified as very good, and the soil profiles P70 and P52, classified as good. Figure 4 presents a validated map of soil degradation.

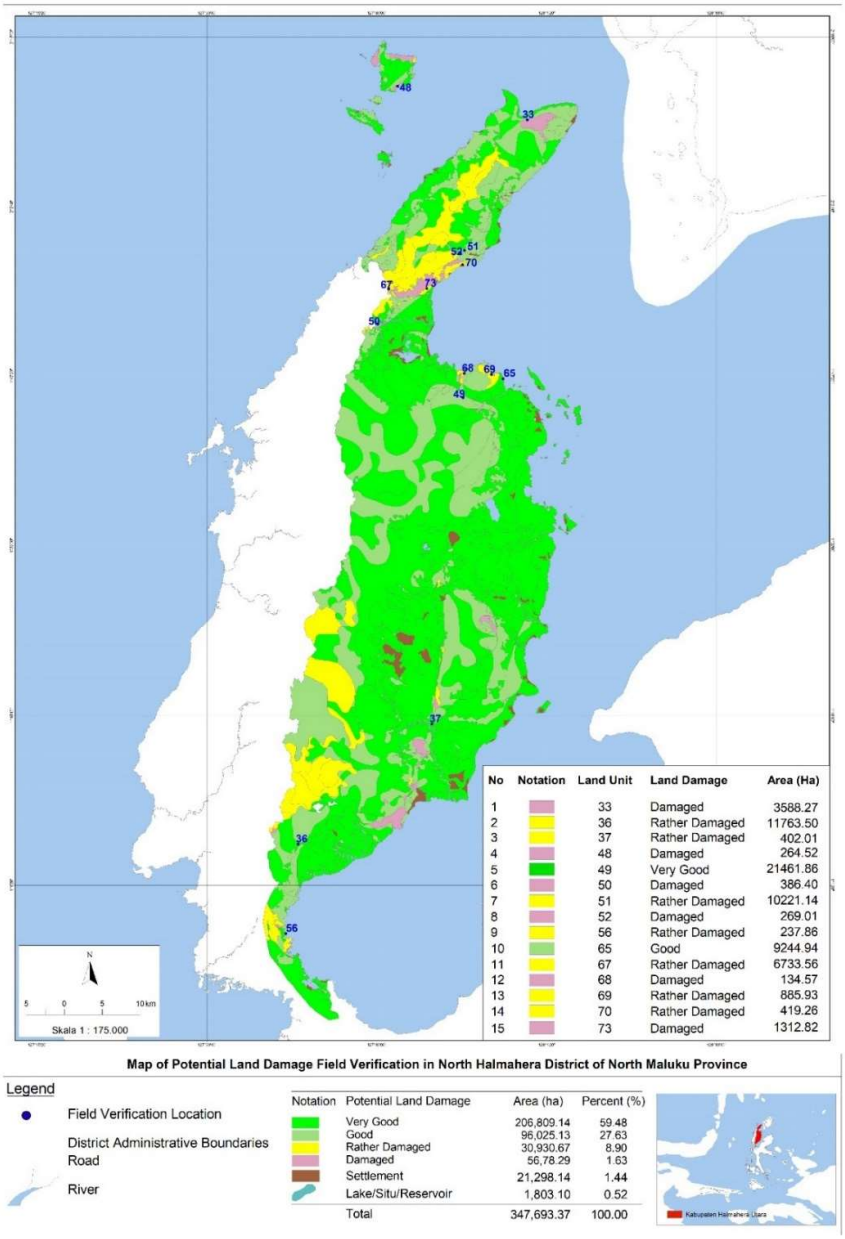

Figure 4. Map of actual soil degradation.

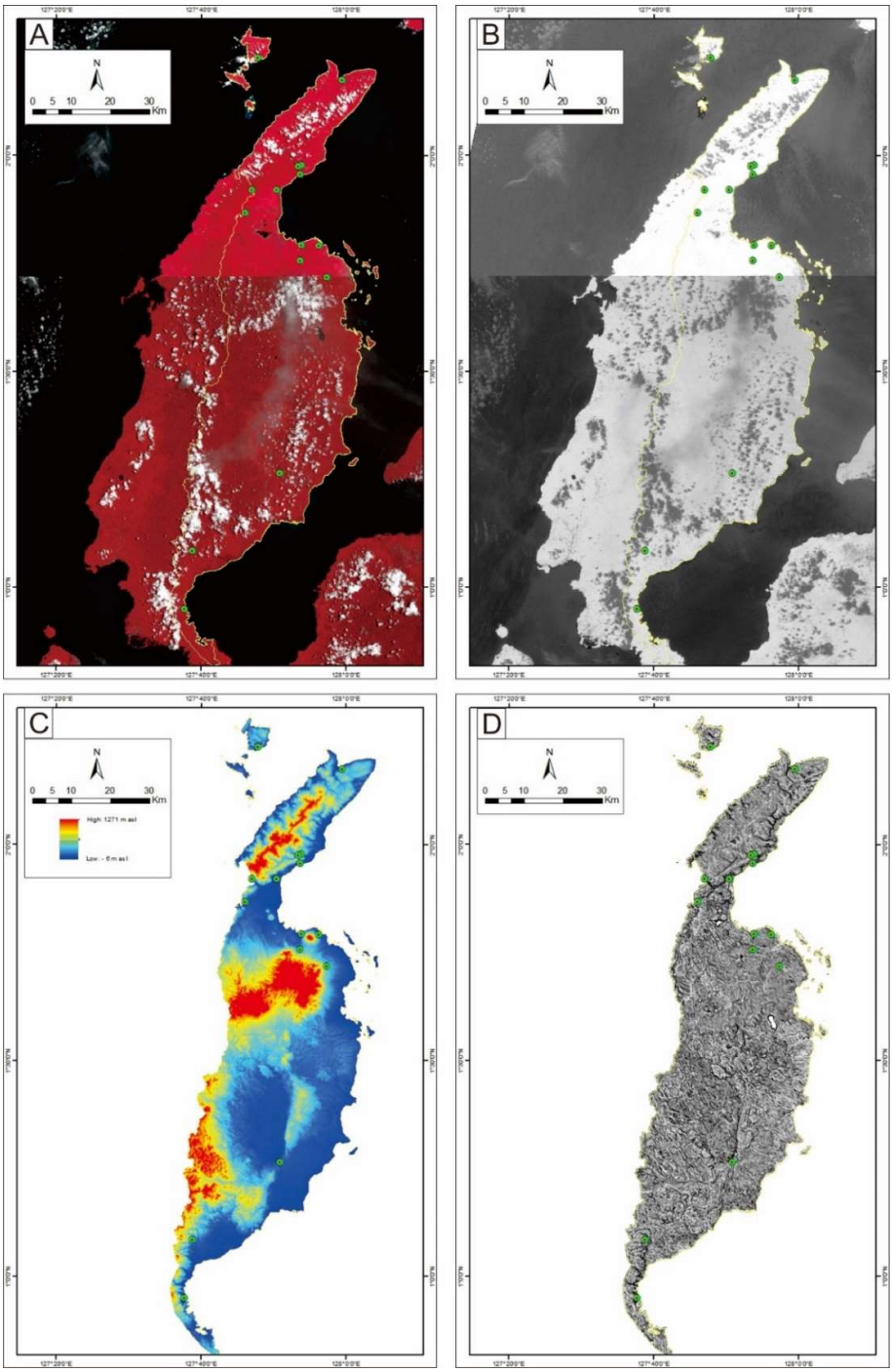

Figure 5. Sentinel 2A and SRTM image processing (A) vegetation (B) Normalized Difference Vegetation Index (C) Digital Elevation Model (D) Terrain Ruggedness Index.

The assessment of the soil degradation index is related to land use and topography. Land uses such as forest, mixed garden, and moor have a diversity of plants with different spacing (Banday et al., 2019; Han et al., 2019). Each plant has a vegetation canopy with a small to large diameter, both of which determine the percentage of vegetation cover to the soil surface. Land use in the form of forests usually has dense vegetation cover, where a large diversity of plants with a tight spacing can cover the soil surface. Meanwhile, mixed and dry gardens have different vegetation canopies, depending on the plants being cultivated (Wessels et

al., 2004). Vegetation cover can reduce the impact of soil erosion and degradation (Wang et al., 2021). NDVI assessments on Sentinel 2A images are commonly used to determine vegetation cover, even to soil conditions under vegetation stands. The presence of vegetation parts and the results of the NDVI analysis are shown in Figures 5A and 5B, respectively. The red colour in Figure 5A is the vegetation density. The portions that appear black in Figure 5B tend to have lower NDVI pixel values than those in white (Table 6). The higher the NDVI value will indicate that the vegetation cover tends to be dense (Xu et al., 2011). Soil degradation is also controlled by topographic indicators such as slope and height difference (Nascimento et al., 2021). The slope is local in the geomorphological zone of the land, while the height difference can be regional. Several researchers previously used the TRI assessment to determine height differences (Gebresamuel et al., 2010; Krenz et al., 2019). Figure 5C shows the DEM data with a maximum height of 1271 m asl (above sea level), and Figure 5D shows the results of the TRI analysis. The white colour in Figure 5D shows that the TRI pixel value tends to be higher than the black colour (Table 6).

The higher TRI value indicates that the area has a relatively rough terrain (Rodríguez-Caballero et al., 2012).

Table 6. Pixel values on NDVI and TRI.

Soil Profile	Normalized Difference Vegetation Index (NDVI)	Terrain Ruggedness Index (TRI)
P65	0.740	0.551
P69	0.689	0.379
P68	0.643	0.186
P49	0.781	0.531
P50	0.623	0.535
P33	0.649	0.344
P70	0.661	0.318
P51	0.581	0.331
P52	0.655	0.258
P73	0.557	0.322
P48	0.573	0.447
P67	0.634	0.411
P37	0.694	0.592
P56	0.696	0.358
P36	0.786	0.568

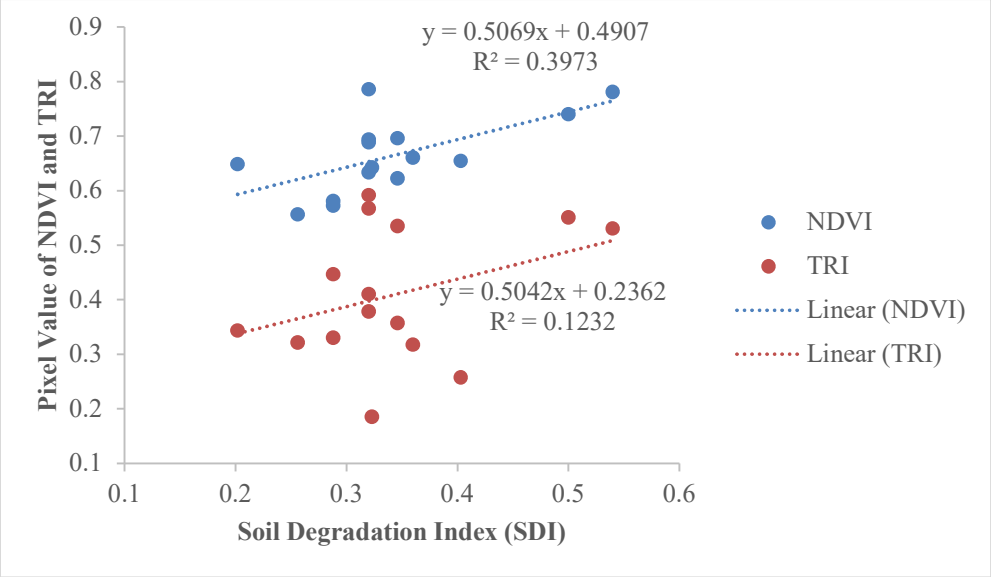

Figure 6. Relationship of SDI with NDVI and TRI.

The relationship of soil degradation index with vegetation (NDVI) and topography (TRI) is presented in Figure 6, in which those factors have a positive linear relationship. The linear equation of the soil degradation index with NDVI and TRI is y = 0.5069x + 0.4907 and y = 0.5042x + 0.2362, respectively. Soil degradation occurs in areas where vegetation tends to be sparse, and the topography tends to be rough, as shown in the structural hills and karst areas. Although soil erosion and soil degradation often occur at low NDVI values, this condition also depends on the characteristics of the surface soil. Most erosion occurs on surface soils that are easily dispersed due to their low content of organic matter or less stable soil aggregates (Ma et al., 2020). The importance of vegetation density, in addition to protecting against rain, is increasing the content of organic matter through the supply of leaf litter (Maraseni and Pandey

2014; Zhang et al., 2019) and creating a microenvironment for microorganisms and soil fauna to live under standing vegetation (Frouz et al., 2008). The interaction between soil microorganisms and fauna with organic matter can also improve soil physical properties, such as increasing soil aggregate stability (Jensen et al., 2020; Mirchooli et al., 2020).

Conclusion

Improper land use accompanied by a lack of conservation measures on steep slopes are factors that trigger soil degradation. Degraded soil is indicated by the presence of a lot of surface rock, relatively shallow solum, and poor physicochemical properties, such as a high percentage of sand, acidic pH, and high electrical conductivity. The thickness of the A horizon and the organic C content of the soil gradually decreases along with the rate of soil degradation that is getting more and more damaged, while chemical properties such as total N, potential P, potential K, and CEC show varying patterns. The level of vegetation cover and topographical surface roughness are important factors in determining degraded and non-degraded soils. Degraded soils can be revitalized by paying attention to the soil morphological properties, soil physicochemical properties, slope, and the selection of plant species with certain functions.

Acknowledgement

The authors would like to thank the North Maluku Province Government for funding and facilitating research amid the COVID-19 pandemic.

References

Aini, L.N., Soenarminto, B.H., Hanudin, E. and Sartohadi, J. 2019. Plant nutritional potency of recent volcanic materials from the southern flank of mt. Merapi, Indonesia. *Bulgarian Journal of Agricultural Science* 25:527-533.

Aini, L.N., Sunarminto, B.H., Hanudin, E. and Sartohadi, J. 2018. Soil morphogenesis diversity at the southern flank of Merapi Volcano, Indonesia five years post-eruption. *Indian Journal of Agricultural Research* 52:472-480, doi:10.18805/ijare.a-325.

Aji, K., Maas, A. and Nurudin, M. 2020. Relationship between soil morphology and variability of upland degradation in Bogowonto Watershed, Central Java, Indonesia. *Journal of Degraded and Mining Lands Management* 7(3):2209-2219, doi:10.15243/jdmlm. 2020.073.2209.

Banday, M., Bhardwaj, D.R. and Pala, N.A. 2019. Influence of forest type, altitude and NDVI on soil properties in forests of North Western Himalaya, India. *Acta Ecologica Sinica* 39(1):50-55, doi:10.1016/j.chnaes.2018.06.001.

Chaplot, V., Giboire, G., Marchand, P. and Valentin, C. 2005. Dynamic modelling for linear erosion initiation and development under climate and land-use changes in northern Laos. *Catena* 63(2):318-328, doi:10.1016/j.catena.2005.06.008.

Frouz, J., Prach, K., Pižl, V., Háněl, L., Starý, J., Tajovský, K., Materna, J., Balík, V., Kalčík, J. and Řehounková, K. 2008. Interactions between soil development, vegetation and soil fauna during spontaneous succession in post mining sites. *European Journal of Soil Biology* 44(1):109-121, doi:10.1016/j.ejsobi.2007.09.002.

Gebresamuel, G., Singh, B.R. and Dick, Ø. 2010. Land-use changes and their impacts on soil degradation and surface runoff of two catchments of Northern Ethiopia. *Acta Agriculturae Scandinavica Section B: Soil and Plant Science* 60:211-226, doi:10.1080/09064710902821741.

Han, J.C., Huang, Y., Zhang, H. and Wu, X. 2019. Characterization of elevation and land cover dependent trends of NDVI variations in the Hexi region, northwest China. *Journal of Environmental Management* 232:1037-1048, doi:10.1016/j.jenvman.2018.11.069.

Higginbottom, T.P. and Symeonakis, E. 2014. Assessing land degradation and desertification using vegetation index data: Current frameworks and future directions. *Remote Sensing* 6(10):9552-9575, doi:10.3390/rs6109552.

Jensen, J.L., Schjønning, P., Watts, C.W., Christensen, B.T., Obour, P.B., and Munkholm, L.J. 2020. Soil degradation and recovery - Changes in organic matter fractions and structural stability. *Geoderma* 364:114181, doi:10.1016/j.geoderma.2020.114181.

Jie, C., Jing-zhang, C., Tan, M. and Zi-tong, G. 2002. Soil degradation: a global problem endangering sustainable development. *Journal of Geographical Sciences* 12(2):243-252, doi:10.1007/bf02837480.

Khaled, H. and Fawy, H.A. 2011. Effect of different levels of humic acids on the nutrient content, plant growth, and soil properties under conditions of salinity. *Soil and Water Research* 6(1):21-29, doi:10.17221/4/2010-swr.

Kooch, Y., Mehr, M.A. and Hosseini, S.M. 2020. The effect of forest degradation intensity on soil function indicators in northern Iran. *Ecological Indicators* 114:106324, doi:10.1016/j.ecolind.2020.106324.

Koutný, L., Skoupil, J. and Veselý, D. 2014. Physical characteristics affecting the infiltration of high intensity rainfall into a soil profile. *Soil and Water Research* 9(3):104-110, doi:10.17221/93/2013-swr.

Krenz, J., Greenwood, P. and Kuhn, N. J. 2019. Soil degradation mapping in drylands using Unmanned Aerial Vehicle (UAV) data. *Soil Systems* 3(2): 33, 1-19, doi:10.3390/soilsystems3020033.

Li, H., Yang, X. and Zhang, K. 2021. Understanding global land degradation processes interacted with complex biophysics and socioeconomics from the perspective of the Normalized Difference Vegetation Index (1982-2015). *Global and Planetary Change* 198(17):103431, doi:10.1016/j.gloplacha.2021.103431.

Li, Z., Lun, F., Liu, M., Xiao, X., Wang, C., Wang, L., Xu, Y., Qi, W. and Sun, D. 2021. Rapid diagnosis of agricultural soil health: A novel soil health index based on natural soil productivity and human management. *Journal of Environmental Management* 277:111402, doi:10.1016/j.jenvman.2020.111402.

Ma, L., Wang, Q. and Shen, S. 2020. Response of soil aggregate stability and distribution of organic carbon to alpine grassland degradation in Northwest Sichuan. *Geoderma Regional* 22:e00309, doi:10.1016/j.geodrs.2020.e00309.

Maraseni, T.N. and Pandey, S.S. 2014. Can vegetation types work as an indicator of soil organic carbon? An insight from native vegetations in Nepal. *Ecological Indicators* 46:315-322, doi:10.1016/j.ecolind.2014.06.038.

Mirchooli, F., Kiani-Harchegani, M., Darvishan, A.K., Falahatkar, S. and Sadeghi, S.H. 2020. Spatial distribution dependency of soil organic carbon content to important environmental variables. *Ecological Indicators* 116:106473, doi:10.1016/j.ecolind.2020.106473.

Mujiyo, Sumarno, Sudadi, and Murti, R. W. 2020. Assessment of soil degradation in Pitu District, Ngawi Regency. *Journal of Degraded and Mining Lands Management* 7(2):2049-2057, doi:10.15243/jdmlm. 2020.072.2049.

Nascimento, C.M., de Sousa Mendes, W., Quiñonez Silvero, N.E., Poppiel, R. R., Sayão, V.M., Dotto, A.C., Valadares dos Santos, N., Accorsi Amorim, M.T. and Demattê, J.A.M. 2021. Soil degradation index developed by multitemporal remote sensing images, climate variables, terrain and soil atributes. *Journal of Environmental Management* 277:111316, doi:10.1016/j.jenvman.2020.111316.

Noviyanto, A., Purwanto, P., Minardi, S. and Supriyadi, S. 2017. The assessment of soil quality of various age of land reclamation after coal mining: a chronosequence study. *Journal of Degraded and Mining Lands Management* 5(1):1009-1018, doi:10.15243/jdmlm.2017.051.1009.

Noviyanto, A., Sartohadi, J. and Purwanto, B.H. 2020. The distribution of soil morphological characteristics for landslide-impacted Sumbing Volcano, Central Java - Indonesia. *Geoenvironmental Disasters* 7:1-19.

Núñez-Delgado, A., Zhou, Y., Anastopoulos, I. and Shaaban, M. 2020. Editorial: New Research on Soil Degradation and Restoration. *Journal of Environmental Management* 269(3):110851, doi:10.1016/j.jenvman.2020.110851.

Rodríguez-Caballero, E., Cantón, Y., Chamizo, S., Afana, A. and Solé-Benet, A. 2012. Effects of biological soil crusts on surface roughness and implications for runoff and erosion. *Geomorphology* 145-146(1):81-89, doi:10.1016/j.geomorph.2011.12.042.

Sartohadi, J., Pulungan, N.A.H.J., Nurudin, M. and Wahyudi, W. 2018. The ecological perspective of landslides at soils with high clay content in the middle Bogowonto watershed, Central Java, Indonesia. *Applied and Environmental Soil Science* 2018:1-9, doi:10.1155/2018/2648185.

Schoeneberger, P.J., Wysocki, D.A., Benham, E. C. and Soil Survey Staff. 2012. Field Book for Describing and Sampling Soils. In Natural Resources Conservation Service, National Soil Survey Center, USDA. Lincoln, NE.

Sun, W., Shao, Q., Liu, J. and Zhai, J. 2014. Assessing the effects of land use and topography on soil erosion on the Loess Plateau in China. *Catena* 121:151-163, doi:10.1016/j.catena.2014.05.009.

van Reeuwijk, L.P. 2002. Procedures for soil analysis. International Soil Reference and Information Centre. Den Haag: Netherlands.

Wang, Z., Lyu, L., Liu, W., Liang, H., Huang, J. and Zhang, Q.-B. 2021. Topographic patterns of forest decline as detected from tree rings and NDVI. *Catena* 198:105011, doi*:*10.1016/j.catena.2020.105011.

Wessels, K.J., Prince, S.D., Frost, P.E., and van Zyl, D. 2004. Assessing the effects of human-induced land degradation in the former homelands of northern South Africa with a 1 km AVHRR NDVI time-series. *Remote Sensing of Environment* 91:47-67, doi:10.1016/j.rse.2004.02.005.

Widiatiningsih, A., Mujiyo, and Suntoro. 2018. Study of Soil Degradation Status at Jatipurno District, Keduang Sub-Watersheds, Wonogiri Regency, Central Java. *Sains Tanah - Journal of Soil Science and Agroclimatology* 15(1):1-14, doi:10.15608/stjssa.v15i1.21616.

Xu, W., Gu, S., Zhao, X.Q., Xiao, J., Tang, Y., Fang, J., Zhang, J. and Jiang, S. 2011. High positive correlation between soil temperature and NDVI from 1982 to 2006 in alpine meadow of the Three-River Source Region on the Qinghai-Tibetan Plateau*. International Journal of Applied Earth Observation and Geoinformation* 13(4):528-535, doi:10.1016/j.jag.2011.02.001.

Yengoh, G.T., Dent, D., Olsson, L., Tengberg, A.E. and Tucker III, C.J. 2015. Use of the Normalized Difference Vegetation Index (NDVI) to Assess Land Degradation at Multiple Scales. Springer: New York.

Zhang, Y., Guo, L., Chen, Y., Shi, T., Luo, M., Ju, Q. L., Zhang, H. and Wang, S. 2019. Prediction of soil organic carbon based on Landsat 8 monthly NDVI data for the Jianghan Plain in Hubei Province, China. *Remote Sensing* 11(14):1683, doi:10.3390/rs11141683.

Zhumanova, M., Mönnig, C., Hergarten, C., Darr, D. and Wrage-Mönnig, N. 2018. Assessment of vegetation degradation in mountainous pastures of the Western Tien-Shan, Kyrgyzstan, using eMODIS NDVI. *Ecological Indicators* 95:527-543, doi:10.1016/j.ecolind.2018.07.060.